Chapter 4
2DOF Control Design for Nanopositioning

Chibum Lee, Gayathri Mohan, and Srinivasa Salapaka

Abstract. This chapter will focus on control systems theoretic analysis and synthesis that significantly expand the range of performance specifications and positioning capabilities of scanning probe microscopes (SPMs). We will present a systems theory framework to study fundamental limitations on the performance of one and two degree-of-freedom (DOF) control designs for nanopositioning systems. In particular, this chapter will present, compare, and analyze optimal-control methods for designing two-degree-of-freedom (2DOF) control laws for nanopositioning. The different methods are motivated by various practical scenarios and difficulty in achieving simultaneously multiple performance objectives of resolution, bandwidth, and robustness by tuning-based or shaping of open-loop-plants based designs. The analysis shows that the primary role of feedback is providing robustness to the closed-loop device whereas the feedforward component is mainly effective in overcoming fundamental algebraic constraints that limit the feedback-only designs. Experimental results indicate substantial improvements (over 200% in bandwidth) when compared to optimal feedback-only controllers.

4.1 Introduction

Positioning of one component with respect to the other with high precision is a pivotal requirement in many micro/nano-scale studies and applications. For instance ultra-high precision positioning systems are crucial to auto focus systems in optics (26), disk spin stands and vibration cancellation (16; 34; 9) in disk drives, wafer and mask positioning in microelectronics (39; 40; 37), piezo hammers in precision mechanics (19), cell penetration and micro dispensing devices in medicine and biology (24), and to the large class of studies and applications enabled by scanning probe microscopes (SPMs). Recently, there is an added impetus on design of nanopositioning systems since they form the bottleneck in terms of speed and accuracy of most

Chibum Lee · Gayathri Mohan · Srinivasa Salapaka
University of Illinois, Urbana Champaign
e-mail: {clee62,gmohan2,salapaka}@illinois.edu

E. Eleftheriou & S.O.R. Moheimani (Eds.): Cntrl. Tech. for Emerging Micro/Nanoscale Sys. LNCIS 413, pp. 67–82.
springerlink.com

devices for nano-investigation, especially in SPMs. For example, there is considerable interest in designing positioning systems for atomic force microscopes (AFMs), since the positioning resolution and tracking bandwidth of positioning systems is typically few orders less than the imaging resolution and bandwidth that micro-cantilever probe provides. Besides high precision positioning, most nano-scientific studies and applications impose severe demands on the tracking bandwidth and reliability in terms of repeatability of experiments. High tracking bandwidth is required since many studies, especially in biology and material science, require assaying matter with nanoscale precision over areas with characteristic lengths that are typically three orders or more. Repeatability of experiments is essential for validation of the underlying studies. This requirement translates to robustness of positioning systems to modeling uncertainties and operating conditions. Devices that are insensitive to (robust to) diverse operating conditions give repeatable measurements, and are hence reliable.

Typical nanopositioning systems comprise of a flexure stage that provides frictionless motion through elastic deformation, an actuator, typically made from piezoelectric material that provides the required force to deform the flexure stage and/or sensing system along with the control system. The main challenges to the design of robust broadband nanopositioning systems come from flexure-stage dynamics that limit the bandwidth of the positioning stage, from nonlinear effects of piezo-actuation such as hysteresis and creep that are difficult to model, and from sensor noise management issues in control feedback that can potentially hamper the tracking-resolution of the device.

The existing literature on designs for improving nanopositioning systems can largely be characterized as those that aim at redesigning the flexure stage mechanisms and those that propose new control methods for existing stages (28; 6). The most common redesign approach is to design smaller and stiffer flexure stages which result in higher resonance frequencies, and therefore provide better tracking-bandwidths (30; 17). However, the downside of this approach is that the resulting smaller, stiffer devices have reduced traversal ranges. The control approaches for better positioning performance can be broadly classified into feedforward and feedback control. A comprehensive review of these designs and their success in increasing positioning resolution is presented in (28; 6). Many of these designs attenuate the hysteresis and creep effects, common in piezo-actuated positioning systems, by carefully modeling these phenomena and compensating them through model-inversion based control designs (13; 36; 11; 4). However, the piezoelectric nonlinearities are sensitive even to small changes in operating conditions such as, ambient temperature, residual polarization in piezo-actuators, and the reference point about which the flexure stage is calibrated; thus making it difficult to estimate accurately their effects and compensate for them. Therefore, many of these designs result in devices that are sensitive to experimental conditions and do not guarantee repeatability of experiments.

Feedback-based control design offers significant compensation against the nonlinear effects of the piezoelectric actuator without explicit incorporation of their models (27; 28). With a careful feedback design, the nonlinear effects of

piezo-actuation can be robustly attenuated even when the measurements are noisy; that is, the net gains in resolution from the suppression of unmodeled piezoelectric effects can be made significantly larger when compared to the negative effects of feeding back noisy measurements (5). Some of these designs have been reviewed in (28). The feedback-only control designs show considerable improvements in positioning resolution, tracking bandwidth, and reliability of positioning systems, however are limited by certain algebraic structure and hardware constraints. These improvements as well as limitations can be explained by analyzing the control block diagram schematic of a typical feedback-only nanopositioning system shown in Figure 4.1. In terms of this diagram, the tracking error is given by $e = Sr + Tn$ where $r, n, S = 1/(1+GK)$, and $T = GK/(1+GK)$ represent the reference, the measurement noise, the sensitivity and the complementary sensitivity transfer functions. Since the complementary sensitivity transfer function T determines the effect of the measurement noise on the tracking error, high-resolution positioning objective requires the control design K to be such that the magnitude $|T|$ is small over the range of frequencies where noise is dominant; more specifically, small values of the roll-off frequency (ω_T) of T guarantee smaller bandwidth of T and therefore good resolution. On the other hand, designing the control K to achieve small values of $|S|$ over large frequency ranges results in a large tracking bandwidth. However the control design K is constrained by the feedback-only structure of the block diagram 4.1(a). For instance, the algebraic limitation $S(j\omega) + T(j\omega) = 1$ at all frequencies ω implies that no control design can achieve small values for the sensitivity and complementary sensitivity simultaneously at the same frequency. A control framework discussed in (21) establishes and quantifies the trade-offs between the performance objectives, and suggests feedback controller designs when feasible.

The Bode integral law (3; 10) poses another fundamental constraint on achieving the performance objectives in a nanopositioning system. According to this law the integral $\int_0^\infty \log|S(j\omega)|d\omega = 0$, for any stable system, relative degree greater than or equal to two (the relative degree condition is generally true for most positioning system models) (35). In a typical positioning system, in fact this limitation holds over a finite frequency range. This restriction implies that any control design that achieves small sensitivity function S (for small tracking error) at a certain frequency range necessarily implies that it will result in large values of S (high-tracking

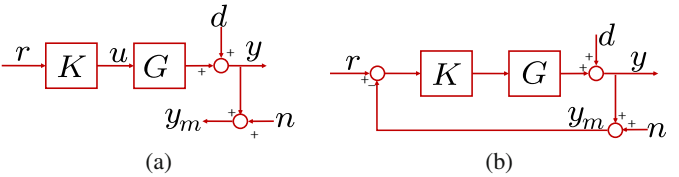

Fig. 4.1 Block diagram schematics for nanopositioning systems: The controller acts only on the reference input signal in open-loop nanopositioning systems shown in (a) while it has access to the difference between the reference and the position y in the closed-loop (feedback-only) positioning system as shown in (b)

error as well as low robustness to modeling uncertainties) at some other frequency ranges. Another important fundamental limitation on control design with respect to the nanopositioning systems is that the complementary sensitivity bandwidth (ω_T) is greater than the bandwidth ω_b of the sensitivity function. Since ω_b signifies tracking bandwidth and ω_T noise-rejection bandwidth, this limitation works against the performance objectives. Feedback controller designs in (31; 27; 33; 2) demonstrate robustness to modeling uncertainties using H_∞ control techniques, and also address the problem of simultaneously achieving the performance objectives. In (7), a multi-input multi-output control design approach is shown that aims to decouple the different positioning directions, and establish a trade-off between the bandwidth and robustness needs.

Some control schemes that combine both the feedforward and feedback techniques are referred to as 2DOF designs. In (14), iterative learning control (ILC) is coupled with feedback control to demonstrate improvements over purely feedback based designs. An inversion based feedforward controller, to compensate for hysteresis effects, along with a feedback controller for pole placement are used in (1) to achieve better tracking.

4.2 Two Degree-of-Freedom Design

The 2DOF control design is analogous to a generalized version of feedback control where the reference inputs and the measurements are processed independently by the controller. The 2DOF controller can take several structures as depicted in Figure 4.2.

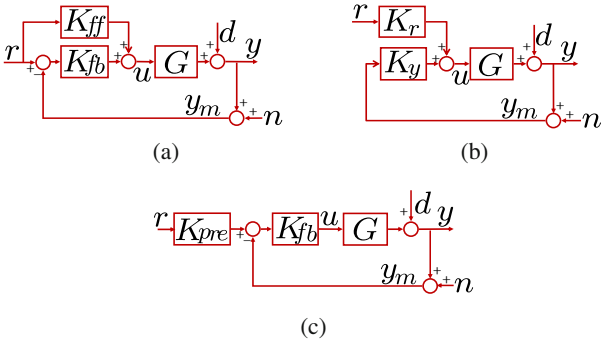

Fig. 4.2 2DOF control architectures: (a) The feedforward-feedback scheme where the actuation signal $u = K_{ff}r + K_{fb}(r - y_m)$, (b) another scheme where $u = K_r r + K_y y_m$, and (c) prefilter architecture where $u = K_{fb}(K_{pre}r - y_m)$. The schemes (a) and (b) are equivalent as control designs in that one can be retrieved exactly in terms of the other. Practical implementable designs for controllers in (a) and (b) can easily be derived from control design in (c), however the vice-versa may require certain factorization procedures.

We primarily consider the 2DOF design shown in Figure 4.2(a) where the control input $u = K_{ff}r + K_{fb}(r - y)$. In this design, the transfer function from d to y that characterizes the robustness to modeling uncertainties is determined by the sensitivity function $S = (I + GK_{fb})^{-1}$, and the transfer function from n to y that characterizes resolution is determined by the complementary sensitivity function $T = (I + GK_{fb})^{-1}GK_{fb}$. Although these characteristics are similar to feedback-only design, the transfer function from r to y and from n to y are distinct and can be designed independently in 2DOF design. The 2DOF design achieves better trade-offs between performance objectives owing to this increased freedom in design. The transfer functions from r to y and r to e are denoted respectively by $S_{er} = S(T - GK_{ff})$ and $T_{yr} = SG(K_{ff} + K_{fb})$. The closed-loop signals namely position, tracking error and control signal, in terms of the new transfer functions S_{er} and T_{yr} are given by, $y = T_{yr}r - Tn + Sd$, $e = S_{er}r + Tn - Sd$, $u = S(K_{ff} + K_{fb})r - SK_{fb}n - SK_{fb}d$ respectively.

Good tracking, a primary performance objective in nanopositioning problems, can be achieved by making the tracking error ($e = S_{er}r + Tn - Sd$) small, which is effected by designing S_{er}, T and S to be small in frequency ranges where the signals r, n and d are dominant respectively. Designing $|T|$ to have small roll-off frequency and high roll-off rates ensures good resolution, keeping $|S_{er}|$ small over large frequency ranges helps achieve large bandwidth and designing the peak magnitude value of S to be close to 1 improves robustness to modeling uncertainties. Here, the norm $||S||_\infty$ gives a measure of the robustness and higher its value lower will be the robustness.

Even though 2DOF control designs provide for larger space of achievable performance specifications over feedback-only designs, they also are constrained by fundamental limitations, both practical and algebraic. Since robustness to modeling uncertainties, and positioning resolution in these designs are still decided by feedback-only transfer functions (S and T respectively), constraints such as Bode-integral law also limit the achievable performance in 2DOF designs.

4.2.1 Feedforward Control Design for Fixed Feedback System

Commercially available nanopositioning systems are typically fitted with pre-designed feedback controllers. These feedback controllers K_{fb} are often not accessible for modification or re-design by users. However, in such cases it is possible to append the system with a feedforward controller in the form of a prefilter on the reference signal (see Figure 4.3). This feedforward component K_{pre} can be designed such that the closed-loop positioning transfer function matches a desired transfer function T_{ref}. The target transfer function T_{ref} is chosen such that it reflects the desired performance objectives such as good resolution and high tracking bandwidth. Additionally, desired transient characteristics including settling times and overshoots, can be attained by choosing an appropriate T_{ref}. Now since the closed-loop transfer function is driven to behave like T_{ref}, it inherits the transient characteristics too.

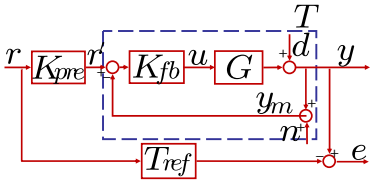

Fig. 4.3 Model matching through prefilter problem

The closed-loop transfer function of the positioning system is given by TK_{pre}. The transfer functions T_{ref} and T are typically stable and proper. A mismatch transfer function $E = T_{ref} - TK_{pre}$ is defined that captures the error between the actual and desired transfer functions. Subsequently, the feedforward component K_{pre} is deduced by posing a minimization problem on the mismatch transfer function E (in the $||.||_\infty$ sense). Small values of $\|E\|_\infty$ guarantees small values for mismatch error signal (see Figure 4.3) given by

$$e = T_{ref} r - y = (T_{ref} - TK_{pre})r. \tag{4.1}$$

This minimization problem at hand becomes trivial if T is a minimum phase transfer function, that is if it has only stable zeros. In this case, the solution K_{pre} can be deduced as $T^{-1}T_{ref}$. However, typical nanopositioning systems are flexure-based with non-collocated actuators and sensors, which give rise to non-minimum phase zeros of T. In such cases, an alternate interpretation of the model matching problem is considered. The model matching problem is analogous to minimizing the parameter γ such that $\|T_{ref} - TK_{pre}\|_\infty \leq \gamma$. If the optimal solution exists the minimum is given by $\gamma = \gamma_{opt}$ for some stable K_{pre}. A further re-formulation of this problem is to find a stable K_{pre} such that $\|E_\gamma\|_\infty \leq 1$, where $E_\gamma = \frac{1}{\gamma}(T_{ref} - TK_{pre})$ for $\gamma > 0$. For stable K_{pre}, the quantity E_γ satisfies the interpolating conditions $E_\gamma(z_i) = \frac{1}{\gamma}T_{ref}(z_i)$ for every non-minimum phase zero z_i of the scanner G. The feedforward component K_{pre} can then be obtained by solving this optimal-control problem by using the Nevanlinna Pick interpolation theory (8).

In Figure 4.4, a 2DOF design comprising a pre-designed feedback controller (designed using $\mathscr{H}_\infty$ optimal framework) and a prefilter (designed using the Nevanlinna-Pick solution) is presented. Its performance is compared to that of the pre-designed feedback-only controller. Since both the 2DOF and feedback-only designs use the same feedback components the resolution and robustness to modeling uncertainties are identical for both cases. Therefore the comparison is made by means of the corresponding sensitivity transfer functions S and S_{er} (refer Figure 4.4), which represent the transfer function from the reference signal to the tracking error. The 2DOF controller shows a significant improvement (330%) over the feedback-only design with respect to tracking bandwidth (see (21) for details).

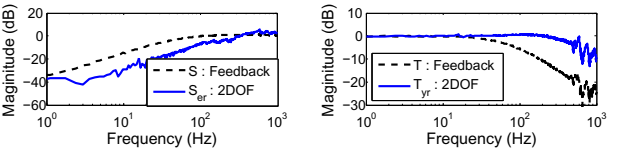

(a) (b)

Fig. 4.4 Comparison of experimentally obtained magnitude of $S(s)$ and $T(s)$ from $\mathscr{H}_\infty$ feedback-only control design (dashed) with $S_{er}(s)$ and $T_{yr}(s)$ from prefilter model matching 2DOF control (solid). The feedforward controller designed using prefilter model matching design achieves over 330% improvement in the tracking bandwidth of the closed-loop design. The robustness and resolution are determined by the feedback components S and T, and therefore remain the same for the two cases.

4.2.2 *Improving Robustness to Operating Conditions for Given Feedback System*

The pre-designed feedback-only controllers present in commercial scanners are developed for satisfactory resolution and bandwidth when operated near nominal operating conditions. The flexure based scanners are extremely sensitive to changes in operating conditions such as ambient temperature, humidity and vibrational noise. Therefore, when there are deviations from the nominal operating conditions, the performance of the feedback-only controller K_s tends to deteriorate. The robustness to such uncertainties can be improved by constructing an additional feedback controller over the existing one. One such scheme that uses the Glover-McFarlane method (12; 23) is illustrated in (33) and demonstrates substantial increase in robustness.

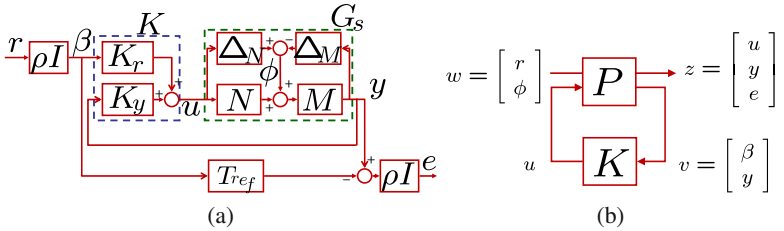

(a) (b)

Fig. 4.5 Control design for model matching and robustness to modeling errors: (a) The signals u, y and e that represent the control signal, the noise component in the position signal, and the mismatch error are chosen as regulated variables z. The transfer function from the reference signal r to these regulated variables z reflects the performance objectives of bounded control signals, noise attenuation, as well as the model matching. The transfer function from the effects of modeling error ϕ to z represents the effect of modeling errors (unmodeled dynamics) on performance objectives. (b) To achieve robust performance, a control design $K = [K_r\ K_y]$ which minimizes the $\mathscr{H}_\infty$-norm of the transfer function from w to z is sought through the optimal control problem.

This section discusses a 2DOF control design comprising of a feedback controller designed for robustness and a feedforward controller for better bandwidth. The 2DOF design adopts the model matching (15; 22) scheme discussed previously where the closed-loop system is targeted to approximate an appropriately chosen model transfer function T_{ref}. Figure 4.5 shows the 2DOF controller along with the plant (scanner) G. The nominal plant model is represented by G_s and the robustness objective implies that the controller based on the optimal solution should be stabilizing for plant models that are in the *neighborhood* of G_s. Using co-prime factorization (38) the nominal plant can be written in terms of functions M and N as $G_s = M^{-1}N$. The vector function $[\Delta_M\ \Delta_N]$ accounts for the unmodeled dynamics in the system. The robustness condition on the plant can now be translated to the set described by G_p,

$$\{G_p | G_p = (M - \Delta_M)^{-1}(N + \Delta_N),\ \text{where}\ \ \|[\Delta_M\ \Delta_N]\|_\infty \leq \gamma^{-1}\}, \tag{4.2}$$

where γ specifies a bound on the uncertainty. An appropriate optimal control problem, in this scenario, seeks a stabilizing controller that is robust to modeling uncertainties in the system and minimizes the mismatch function (difference between the transfer function from r to y and the target transfer function T_{ref}) under a preferred norm. The target transfer function T_{ref} (similar to Section 4.2.1) is chosen to satisfy response characteristics that are desired for the closed-loop transfer function.

The optimal control problem posed minimizes the transfer function $\Phi(K)$ from signals r and ϕ (an exogenous disturbance signal that captures the effects of uncertainties, see Figure 4.5) to the closed-loop variables $[u^T\ y^T\ e^T]^T$ under the $\mathscr{H}_\infty$ norm (21). A weighting factor ρ maybe used to decide the relative emphasis on the robustification aspect over model matching during optimization. Here, minimizing the norm of $\Phi(K)$ ensures that the effect of ϕ on the mismatch (error) signal e is minimized. As a consequence, the mismatch signal becomes insensitive to modeling uncertainties. Also the constraints on the saturation limit of control and the problem of noise attenuation are handled by the inclusion of u and y as regulated variables in the optimal control problem.

In (21) it is shown that this 2DOF design simultaneously achieves good tracking bandwidth and robustness to uncertainties, for the same resolution, which is not feasible with a feedback-only design owing to algebraic constraints (see Section 4.1). The PII controller is a widely prevalent choice for the feedback-only controller in nanopositioning systems. This can be attributed to the ease of implementation and ability of the PII controller to track ramp signals (representative of triangular raster scans). Figure 4.6 compares the performance of the feedback-only controller (PII) and the 2DOF controller in terms of the sensitivity and complementary sensitivity functions of the corresponding closed-loop systems. It is shown that there is over 64% improvement in bandwidth (S_{er} over S). The improvement in robustness is illustrated through comparison of $S(j\omega)$, the value of $||S||_\infty$ is 1.52 for the 1DOF and 1.21 for the 2DOF design. As mentioned earlier, the smaller the value of $||S||_\infty$, higher the robustness.

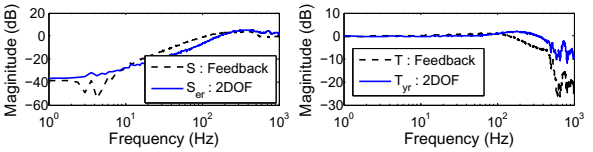

(a) (b)

Fig. 4.6 Comparison of experimentally obtained magnitude of $S(s)$ and $T(s)$ from PII feedback-only control design (dashed) with $S_{er}(s)$ and $T_{yr}(s)$ from 2DOF optimal robust model matching control (solid). The 2DOF optimal robust model matching controller achieves over 64% improvement in the tracking bandwidth.

4.2.3 Simultaneous Feedback and Feedforward Control Design

For the 2DOF design considered in this section, an optimal control problem is cast that simultaneously decides the feedforward and feedback control. It is different from the previous formulations in the sense that the relative duties of feedforward and feedback components are not explicitly specified. The objectives are focused on robust stability, disturbance rejection and noise attenuation. Also, the closed-loop response is designed to mimic a target response $T_{ref}r$ similar to previous sections. The chosen controller configuration is illustrated in Figure 4.7. In order to satisfy the desired objectives, the regulated signals are chosen to be

$$z_m = T_{ref}r - y, \qquad z_s = W_s(r - n - y), \qquad z_t = W_t y,$$

where z_m, z_s, and z_t represent the deviation from target response, the weighted tracking error including noise, and the weighted system output. The objectives therefore require these regulated variables to be small. For higher flexibility in design the transfer functions S and T are weighted by functions W_s and W_t. Following a

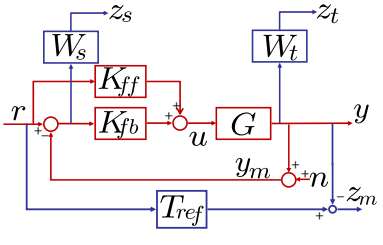

Fig. 4.7 Control design for 2DOF stacked sensitivity with model matching design. The signals z_m, z_s, and z_t represent the deviation from target response, the weighted tracking error with noise, and the weighted system output. The weights W_s and W_t are chosen to reflect the design specifications of robust stability, disturbance rejection and noise attenuation. The target response function T_{ref} is chosen to specify the performance of close loop response to reference signal.

procedure similar to Section 4.2.2, the matrix transfer function from the exogenous inputs, $w = [r^T \;\; n^T]^T$ to the regulated output signals, $z = [z_m^T \;\; z_s^T \;\; z_t^T]^T$ is formulated as

$$\begin{bmatrix} z_m \\ z_s \\ z_t \end{bmatrix} = \underbrace{\begin{bmatrix} T_{ref} - T_{yr} & T \\ W_s S_{er} & -W_s S \\ W_t T_{yr} & -W_t T \end{bmatrix}}_{=\Phi(K)} \begin{bmatrix} r \\ n \end{bmatrix}. \tag{4.3}$$

Now it is possible to pose an optimal control problem to minimize this matrix transfer function under the $\mathscr{H}_\infty$ norm. However, the minimization of this matrix transfer function $\Phi(K)$ also includes minimization of terms such as T, $W_s S_{er}$ and $W_t T_{yr}$ that are unrelated to the specified design objectives. In addition, the algebraic constraints discussed previously ($S + T = I$ and $S_{er} + T_{yr} = I$) impose severe limitations on the feasible controller subspace for the minimization problem. Therefore, instead of casting in terms of the regulated output signals, a different multi-objective approach where the goal is to minimize the transfer functions $T_{ref} - T_{yr}$, $W_s S$ and $W_t T$ is considered. The problem is translated to an optimal control problem with LMI conditions (29).

The problem is reduced to minimizing the transfer functions from r to z_m and from n to $[z_s^T \;\; z_t^T]^T$ and written as

$$\min_{K \in \mathscr{K}} \rho \left\| T_{ref} - T_{yr} \right\|_{\alpha_1} + \left\| \begin{matrix} W_s S \\ W_t T \end{matrix} \right\|_{\alpha_2}, \tag{4.4}$$

where $K = [K_{ff} \;\; K_{fb}]$, $\mathscr{K}$ is the set of stabilizing controllers and the parameter ρ is chosen to decide the relative importance between model matching and robust performance and $\|\cdot\|_{\alpha_i, i \in \{1,2\}}$ can either be the 2-norm or the ∞-norm.

The multi-objective problem can be realized in the generalized control framework as shown in Figure 4.8. The generalized matrix function P in this formulation is given by,

$$\left[\begin{array}{c} z_m \\ z_s \\ z_t \\ \hline r \\ r-n-y \end{array}\right] = \underbrace{\left[\begin{array}{ccc|c} T_{ref} & 0 & -G \\ W_s & -W_s & W_s G \\ 0 & 0 & W_t G \\ \hline I & 0 & 0 \\ I & -I & -G \end{array}\right]}_{=P} \left[\begin{array}{c} r \\ n \\ \hline u \end{array}\right], \tag{4.5}$$

and is denoted in the state space by,

$$P \equiv \left[\begin{array}{c|cc} A & B_w & B \\ \hline C_z & D_{zw} & D_z \\ C & D_w & 0 \end{array}\right]. \tag{4.6}$$

By adopting this scheme, the redundancies in minimization present initially are overcome. If the controller is assumed to take the form

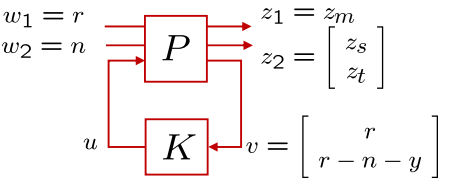

Fig. 4.8 General framework for 2DOF control in Eq. (4.4): The multi-objective optimization problem is to design a controller that minimizes the sum of ρ times the transfer function from w_1 to z_1 and the transfer function from w_2 to z_2. This is in contrast to stacked sensitivity framework that minimizes the transfer function from $w = [w_1^T \; w_2^T]^T$ to $[z_1^T \; z_2^T]^T$.

$$K(s) = [K_{ff}(s) \;\; K_{fb}(s)] \equiv \left[\begin{array}{c|c} A_k & B_k \\ \hline C_k & D_k \end{array}\right], \tag{4.7}$$

then the final closed-loop transfer function can be deduced as,

$$\begin{aligned} \Phi &= \left[\begin{array}{cc|c} A + BD_kC & BC_k & B_w + BD_kD_w \\ B_kC & A_k & B_kD_w \\ \hline C_z + D_zD_kC & D_zC_k & D_{zw} + D_zD_kDw \end{array}\right] \\ &\equiv \left[\begin{array}{c|c} \bar{A} & \bar{B} \\ \hline \bar{C} & \bar{D} \end{array}\right]. \end{aligned} \tag{4.8}$$

In Figure 4.8, the transfer functions from w_i to z_i (for $i = 1, 2$) reflect the performance objectives desired and can be re-written in terms of the transfer function Φ in Eq. (4.3) as $\Phi_i = L_i \Phi R_i$, where the matrices L_i and R_i are chosen appropriately. The optimization problem in Eq. (4.4) is recast as the following problem,

$$\min \quad \rho\gamma_1 + \gamma_2 \tag{4.9}$$

when subject to the LMIs corresponding to the required performance objectives for Φ_1 and Φ_2. For instance, we could pose $\mathscr{H}_\infty$ performance conditions on these transfer functions in terms of LMIs. Now, the solution can be obtained by using standard convex optimization techniques following which the controller is deduced from the optimal solution (see (20) for details).

Experimental results illustrate that this 2DOF control design leads to 216% improvement in bandwidth over a 1DOF stacked sensitivity optimal control design, for almost the same robustness and resolution (refer Figure 4.10). Figure 4.9(a) shows that S_{er} achieves good tracking over the 1DOF design with good robustness to modeling uncertainties (note the $\|S\|_\infty$ value). Figure 4.9(b) shows the roll-off frequency of T_{yr} as against T from the experiment.

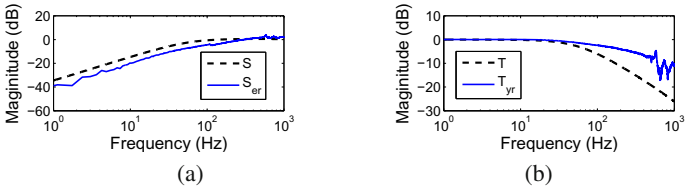

Fig. 4.9 Magnitude of $S_{er}(s)$ and $T_{yr}(s)$ (solid) obtained from experiment with S and T (dashed)

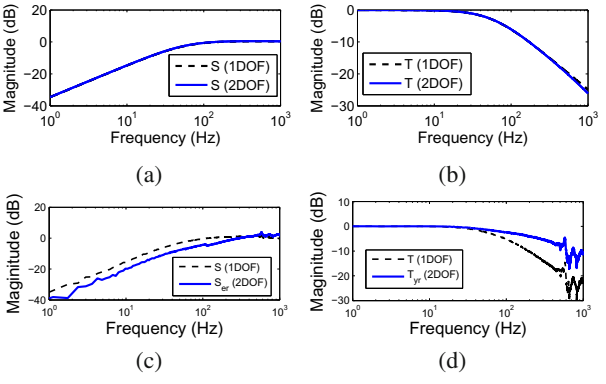

Fig. 4.10 Comparison of $\mathscr{H}_\infty$ feedback-only stacked synthesis and 2DOF multi-objective synthesis control design. (a),(b) $|S|$ and $|T|$ from 1DOF control design (dashed) with $|S|$ and $|T|$ from 2DOF control design (solid). (c),(d) $|S|$ and $|T|$ from 1DOF control design (dashed) with $|S_{er}|$ and $|T_{yr}|$ from 2DOF control design (solid) obtained from experiment. The 2DOF multi-objective synthesis control achieves about 216% improvement in the tracking bandwidth.

4.2.4 Role of Feedforward and Feedback Components

The sensitivity and the complementary sensitivity functions determine the positioning resolution and robustness to modeling uncertainties in both the 1DOF and 2DOF designs. Therefore the direct advantage of the 2DOF design is in its ability to achieve larger tracking bandwidths when compared to 1DOF designs. This advantage also translates to indirect benefits in terms of being able to achieve better trade-offs between the resolution, robustness, and bandwidth objectives. The fundamental limitations that apply to the control design in 1DOF design also apply to the design of the feedback component K_{fb} in the 2DOF design. For instance, the bode integral law described in Section 4.1 does apply to the sensitivity function in 2DOF design and therefore poses a constraint on the design of K_{fb}. The feedforward component on the other hand is not constrained by such limitations, but at the same time does not affect the resolution or the robustness objectives. Therefore to simultaneously achieve the multiple performance objectives, the feedback component plays a primary role as it

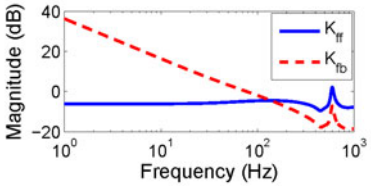

Fig. 4.11 The optimization problem automatically separates the roles of the feedforward and feedback control. The feedback component K_{fb} is dominant in the low frequency region and the feedforward component K_{ff} shows dominance in the higher frequency range.

decides both the resolution and the robustness characteristics in addition to affecting the bandwidth. In this sense, the feedforward component plays a secondary role and is hardly effective in the frequency ranges where feedback component is large (that is where the sensitivity function is small). In fact, the feedforward component K_{ff} becomes prominent only in the frequency ranges where the sensitivity function S can no longer be made small. This division of roles is corroborated by the solutions to the optimal control formulations where both the feedback and feedforward controllers are treated as decision variables with no distinguishing role assigned to them a priori (see Figure 4.11). Therefore the advantage of the feedforward component is primarily in increasing the bandwidth from the corner frequency of S to about the resonance frequencies of the flexure stages. To make the system bandwidth larger than the flexure resonance typically requires a huge control effort and the saturation limit on control becomes a serious limitation.

An analysis of the 2DOF designs show that they achieve specifications that are impossible for the 1DOF designs, that is, some of the fundamental limitations on the 1DOF design do not apply to the 2DOF designs. As stated in Section 4.1, high values of tracking bandwidth ω_{BW} and small values of roll-off frequency (ω_T) of the complementary sensitivity function T are desired for good tracking and noise attenuation. However, in feedback-only controller design this is not achievable, since ω_{BW} cannot be made higher than ω_T owing to fundamental limitations (35). The 2DOF control design on the other hand, is not bound by such restrictions, as can be seen from the experimental illustrations in the previous sections (in optimal prefilter model matching control based on $\mathscr{H}_\infty$ controller ω_{BW} of 214.5 Hz and ω_T of 60.1 Hz while in 1DOF $\mathscr{H}_\infty$ control design the bandwidth is 49.4 Hz with the same roll-off frequency). Additionally, it is shown using the 2DOF designs in this chapter, it is possible to improve the bandwidth and robustness to modeling uncertainties for a given resolution while fundamental limitations pose restrictions on the feedback-only design to achieve this trade-off.

4.3 Summary

In this chapter the role and design of 2DOF control methods for nanopositioning systems are discussed. It is shown that the trade off imposed by fundamental

limitations in 1DOF can be relaxed through 2DOF control. The control designs when implemented on an AFM give substantial improvements in bandwidth (as high as 330%) for the same resolution and robustness. The experiments demonstrate that 2DOF design presented here achieved design specifications that were analytically (and therefore practically) impossible for feedback-only designs. Here the comparisons have been made to feedback-only designs which by themselves have obtained significant improvements over commercial devices (27). It is shown that the modern control theoretic framework provides an apt platform to quantify and analyze the design objectives of robustness, bandwidth and resolution as well as to design control laws to achieve them. Even though this chapter is focused on nanopositioning, the tools provided in this chapter are applicable to various applications in nanotechnology (25; 32). For instance, these tools have been applied in a variety of contexts in scanning probe microscopy (18). The underlying framework allows for quantification of desired objectives, analysis of fundamental limitations, computing inherent trade-offs between performance objectives, and designing and solving optimal control problems to achieve best feasible performance.

References

[1] Aphale, S.S., Devasia, S., Moheimani, S.O.R.: High-bandwidth control of a piezoelectric nanopositioning stage in the presence of plant uncertainties. Nanotechnology 19(12), 125–503 (2008)

[2] Bashash, S., Jalili, N.: Robust adaptive control of coupled parallel piezo-flexural nanopositioning stages. IEEE/ASME Transactions on Mechatronics 14(1), 11–20 (2009)

[3] Bode, H.: Network Analysis and Feedback Amplifier Design. Van Nostrand Reinhold, New York (1945)

[4] Croft, D., Shedd, G., Devasia, S.: Creep, hysteresis and vibration compensation for piezoactuators: Atomic force microscopy application. In: Proceedings of the Amercian Control Conference, Chicago, IL, pp. 2123–2128 (2000)

[5] Daniele, A., Salapaka, S., Salapaka, M.V., Dahleh, M.: Piezoelectric scanners for atomic force microscopes: design of lateral sensors, identification and control. In: Proceedings of the American Control Conference, San Diego, CA, pp. 253–257 (1999)

[6] Devasia, S., Eleftheriou, E., Moheimani, S.O.R.: A survey of control issues in nanopositioning. IEEE Transactions of Control Systems Technology 15(5), 802–823 (2007)

[7] Dong, J., Salapaka, S., Ferreira, P.: Robust control of a parallel-kinematic nanopositioner. Journal of Dynamic Systems, Measurement, and Control 130, 041007 (2008)

[8] Doyle, J.C., Francis, B.A., Tannenbaum, A.R.: Feedback Control Theory. MacMillan, New York (1992)

[9] Du, C., Xie, L., Teoh, J.N., Guo, G.: An improved mixed $\mathscr{H}_2/\mathscr{H}_\infty$ control design for hard disk drives. IEEE Transactions on Control Systems Technology **13**(5), 832–839 (2005)

[10] Freudenberg, J.S., Looze, D.P.: Right half-plane poles and zeros and design tradeoffs in feedback systems. IEEE Transactions on Automatic Control 30(6), 555–565 (1985)

[11] Ge, P., Jouaneh, M.: Tracking control of a piezoceramic acuator. IEEE Transactions on Control Systems Technology 4(3), 209–216 (1996)

[12] Glover, K., McFarlane, D.: Robust stabilization of normalized coprime factor plant descriptions with $\mathscr{H}_\infty$-bounded uncertainty. IEEE Transactions on Automatic Control 34(8), 821–830 (1989)
[13] Hatch, A.G., Smith, R.C., De, T., Salapaka, M.V.: Construction and experimental implementation of a model-based inverse filter to attenuate hysteresis in ferroelectric transducers. IEEE Transactions on Control Systems Technology 14(6), 1058–1069 (2006)
[14] Helfrich, B.E., Lee, C., Bristow, D.A., Xiaohui, X., Dong, J., Alleyne, A.G., Salapaka, S.: Combined $\mathscr{H}_\infty$-feedback and iterative learning control design with application to nanopositioning systems. In: Proceedings of American Control Conference, Seattle, WA, pp. 3893–3900 (2008)
[15] Hoyle, D.J., Hyde, R.A., Limebeer, D.J.N.: An $\mathscr{H}_\infty$ approach to two degree of freedom design. In: Proceedings of the IEEE Conference on Decision and Control, pp. 1581–1585 (1991)
[16] Jianxu, M., Ang Jr., M.: High-bandwidth macro/microactuation for hard disk drive. In: Proceedings of the SPIE, vol. 4194, pp. 94–102 (2000)
[17] Leang, K., Fleming, A.: High-speed serial-kinematic AFM scanner: Design and drive considerations. In: Proceedings American Control Conference, pp. 3188–3193 (2008)
[18] Lee, C.: Control-systems based analysis and design methos for scanning probe microscopy. Ph.D. thesis, University of Illinois at Urbana-Champaign (2010)
[19] Lee, C., Lin, C., Hsia, C., Liaw, W.: New tools for structural testing: Piezoelectric impact hammers and acceleration rate sensors. Journal of Guidance, Control and Dynamics 21(5), 692–697 (1998)
[20] Lee, C., Salapaka, S., Voulgaris, P.: Two degree of freedom robust optimal control design using a linear matrix inequality optimization. In: 48th IEEE Conference on Decision and Control (December 2009)
[21] Lee, C., Salapaka, S.M.: Robust broadband nanopositioning: fundamental trade-offs, analysis, and design in a two-degree-of-freedom control framework. Nanotechnology 20(3), 035,501 (2009)
[22] Limebeer, D., Kasenally, E., Perkins, J.: On the design of robust two degree of freedom controllers. Automatica 29(1), 157–168 (1993)
[23] McFarlane, D., Glover, K.: A loop shaping design procedure using $\mathscr{H}_\infty$ synthesis. IEEE Transactions on Automatic Control 37(6), 759–769 (1992)
[24] Meldrum, D.R., Pence, W.H., Moody, S.E., Cunningham, D.L., Holl, M., Wiktor, P.J., Saini, M., Moore, M.P., Jang, L.S., Kidd, M., Fisher, C., Cookson, A.: Automated, integrated modules for fluid handling, thermal cycling and purification of DNA samples for high throughput sequencing and analysis. In: Proc. IEEE/ASME International Conference on Advanced Intelligent Mechatronics, vol. 2, pp. 1211–1219 (2001)
[25] Pantazi, A., Sebastian, A., et al.: Probe-based ultrahigh-density storage technology. IBM Journal of Research and Development 52(4/5), 493–511 (2008)
[26] Rihong, Z., Daocai, X., Zhixing, Y., Jinbang, C.: Research on systems for measurements of CCD parameters. In: Proceedings of the SPIE, vol. 3553, pp. 297–301 (1998)
[27] Salapaka, S., Sebastian, A., Cleveland, J.P., Salapaka, M.V.: High bandwidth nanopositioner: A robust control approach. Review of Scientific Instruments 73(9), 3232–3241 (2002)
[28] Salapaka, S.M., Salapaka, M.V.: Scanning probe microscopy. IEEE Control Systems Magazine 28(2), 65–83 (2008)
[29] Scherer, C., Gahinet, P., Chilali, M.: Multiobjective output-feedback control via LMI optimization. IEEE Transactions on Automatic Control 42(7), 896–911 (1997)

[30] Schitter, G., Astrom, K., DeMartini, B., Thurner, P., Turner, K., Hansma, P.: Design and modeling of a high-speed AFM-scanner. IEEE Transactions on Control Systems Technology 15(5), 906–915 (2007)
[31] Schitter, G., Menold, P., Knapp, H.F., Allgower, F., Stemmer, A.: High performance feedback for fast scanning atomic force microscopes. Review of Scientific Instruments 72(8), 3320–3327 (2001)
[32] Sebastian, A., Pantazi, A., et al.: Nanopositioning for probe storage. In: Proceedings of the American Control Conference, Portland, OR, pp. 4181–4186 (2005)
[33] Sebastian, A., Salapaka, S.: Design methodologies for robust nano-positioning. IEEE Transactions on Control Systems Technology 13(6), 868–876 (2005)
[34] Shim, D., Lee, H.S., Guo, L.: Mixed-objective optimization of a track-following controller using linear matrix inequalities. IEEE/ASME Transactions on Mechatronics 9(4), 636–643 (2004)
[35] Skogestad, S., Postlethwaite, I.: Multivariable Feedback Control, Analysis and Design, 2nd edn. John Wiley and Sons, West Sussex (2005)
[36] Smith, R.C., Hatch, A.G., De, T., Salapaka, M.V., del Rosario, R.C.H., Raye, J.K.: Model development for atomic force microscope stage mechanisms. SIAM Journal on Applied Mathematics 66(6), 1998–2026 (2006)
[37] Verma, S., Jong Kim, W., Shakir, H.: Multi-axis maglev nanopositioner for precision manufacturing and manipulation applications. IEEE Transactions on Industry Applications 41(5), 1159–1167 (2005)
[38] Vidyasagar, M.: Control System Synthesis: A Factorization Approach. MIT Press, Cambridge (1985)
[39] White, D., Wood, O.: Novel alignment system for imprint lithography. Journal of Vacuum Science & Technology B 18(6), 3552–3556 (2000)
[40] Zandvliet, M.J., Scherer, C.W., Hol, C.W.J., van de Wal, M.M.J.: Multi-objective $\mathscr{H}_\infty$ control applied to a wafer stage model. In: Proc. 43rd IEEE Conference on CDC Decision and Control, vol. 1, pp. 796–802 (2004)